Rotational Discontinuity in the Magnetopause Boundary Layer for Open Magnetosphere

Yonghui Ma[1], Shu Wang [1], Chao Shen[1], Nian Ren[1], Peng Shao[1], Peng E[2], Y. V. Bogdanova [3], J. L. Burch[4]

[1]School of Science, Harbin Institute of Technology, Shenzhen, 518055, China.

[2] Laboratory for Space Environment and Physical Sciences, Harbin Institute of Technology, Harbin, 150001, China.

[3]Rutherford Appleton Laboratory, Chilton, DIDCOT, Oxfordshire OX11 0QX, United Kingdom

[4]Southwest Research Institute, San Antonio, TX, USA

Corresponding author: Chao Shen (shenchao@hit.edu.cn)

Index Terms:

2740 Magnetospheric Physics: Magnetospheric configuration and dynamics;

2724 Magnetospheric Physics: Magnetopause and boundary layers;

2723 Magnetospheric Physics, 7835 Space Plasma Physics: Magnetic reconnection;

7811 Space Plasma Physics: Discontinuities;

Key points:

1. **The fine magnetic structure of Rotational Discontinuity (RD) at the dayside magnetopause is revealed.**
2. **RD is a very thin layer and usually at the magnetosheath side of the magnetopause.**
3. **The magnetic strength minimums and magnetic field rotates severely in the RD.**

KEYWORDS:

Magnetic field, Magnetopause, Rotational Discontinuties, Magnetic reconnection, Interaction between Solar Wind and Magnetosphere

Running Title: Structure of the Magnetopause BL

Abstract In this paper, we analyzed the fine structure of the rotational discontinuity (RD) in the magnetopause of the open magnetosphere by using the MMS four-point magnetic field measurements. It is found that RD is very common within the magnetopause when reconnection occurs at the magnetopause. Furthermore, RD usually occurs closer to the magnetosheath side of the magnetopause. RD is very thin and its thickness is usually much smaller than 0.1 Re. The magnetic field rotation maximums and magnetic strength minimums within the RD. The radius of curvature of the magnetic field lines reaches its minimum value in the RD (~0.03-0.62 Re). In addition, the radius of curvature of magnetic field line of RD is usually larger than the thickness of RD structure, indicating that the magnetic field lines are partly lying in the RD. Generally，the field-aligned current dominates in the RD.

Plain language summary

The magnetopause is the sharp outer boundary of magnetosphere. It is a key region in space transferring the solar wind mass, momentum and energy into the magnetosphere. In the MHD framework, the magnetopause usually can take either the tangential discontinuity (TD) or rotational discontinuity (RD). As the magnetopause reconnection occurs, it is expected that there is a RD-type magnetopause. However, the fine structure and current distribution of RD remains unclear. In this study, by using the four-point magnetic field measurements from MMS, we studied the fine structure of the RD which is closely related with the reconnection processes. Investigation on the RD structure can enhance our understanding of the interaction between the solar wind and magnetosphere.

1. Introduction

Rotational discontinuities (RDs) are very important structures at Earth's magnetopause, which indicate the magnetosphere becomes open and there could be plasma exchange between solar wind and magnetosphere. RDs are associated with ongoing reconnection at magnetopause on the basis of standard MHD models [*Dungey, 1961; Levy et al., 1964; Sonnerup and Ladley, 1979; Crooker, 1986; Paschmann et al., 2018*]. Simulations have shown that the RDs at magnetopause could be stable and very thin with a scale width of several ion inertial lengths [*Lee et al., 1989；Krauss-Varban et al., 1995*]. Previous researchers have used single S/C exploration data to analyze the features of RDs [*Sonnerup and Ladley, 1974*]. It is found that within the RDs the magnetic strength keeps constant and the magnetic field vector rotates by180°. *Aggson et al. (1983)* found that there is large electric field along the normal of the RDs of magnetopause boundary layer.

A statistical analysis of the structure of Earth's magnetopause was studied by *Chou et al.(2012)*. Their analyses are based on the minimum variance analysis (MVA), the deHoffmann-Teller (HT) frame analysis and the Walen relation. In their study, a total of 328 magnetopause crossings are identified. In 142 out of 328 events both MVA and HT frame analyses yield high quality results which are classified as either tangential discontinuities (TDs) or RD structures based only on the Walen relation. With this criterion, 84% of 142 events are TDs, 12% are RDs, and 4% are uncertain events. As we can see, there are very few examples of RD structure in the Earth's

magnetopause. In recent years, there are few researches on the RD, especially its magnetic field structure and current distribution.

As RD is the product of magnetic reconnection, the study on it is also conducive for the further understanding of magnetic reconnection. Because the magnetospheric magnetic field strength is generally larger than that of magnetosheath, and the magnetospheric plasma densities are much lower, RD at the magnetopause is typically highly asymmetric. Recently, *Haaland et al. (2019)* explored the structure of the flank magnetopause by Magnetospheric MultiScale (MMS) and made a comparison with that in the dayside magnetopause. They found that the flank magnetopause boundary layer is thicker and has lower current density than that in the dayside. However, they have not presented the fine structure of the magnetic field and current distribution.

In this investigation, we apply the magnetic rotation analysis (MRA) approach [*Shen et al., 2007*] to study the properties of RDs at magnetopause boundary layer with MMS 4-point measurements [*Burch et al., 2016*]. The outline of this paper is as follows. Section 2 we will give a brief description of the method [*Shen et al., 2003, 2007*] and the data used. In section 3, the observations of magnetopause boundary layer, especially for the RDs, are presented in detail. We give a statistical analysis and the general feature of RD in Section 4. Section 5 is the discussion and conclusions.

2. Data and Methodology

In this study, magnetic field measurement from Fluxgate Magnetometer [*Russell et al., 2014*] and plasma measurement from Fast Plasma Investigation (FPI) [*Torbert,*

130 *et al. 2015; Pollock et al., 2016*] of MMS are used to identify the magnetopause
131 crossings as well as RD structure in the boundary layer.

132 In this study, we used the methods developed by *Shen et al. (2003, 2007)* to
133 analyze the structure of magnetic field lines using four-point magnetic field
134 observations. Using these approaches, we can also obtain the curvature of the
135 magnetic field lines, gradient of magnetic field strength, rotation rates of magnetic
136 field as well as the current density. For a better understanding of the analysis results in
137 this paper, here we give a discussion of the applied approaches.

138 The curvature calculation method [*Shen et al., 2003*] can be summarized as the
139 followings. The local curvature of one magnetic field line can be defined as

140 $$\vec{\rho}_c = (\vec{b} \cdot \nabla)\vec{b}, \quad (1)$$

141 where $\vec{b}$ is the unit vector of magnetic field $\vec{B}$. This formula can be expanded
142 as

143 $$\rho_{cj} = B^{-2} B_i \nabla_i B_j - B^{-4} B_j B_i B_l \nabla_i B_l, \quad (2)$$

144 where the subscript index *i*, *j*, and *l* (= 1, 2, and 3) denote the three components *x*,
145 *y*, and *z*, respectively. The curvature radius is the reciprocal value of the curvature ρ_c,
146 that is, $R_c = 1/\rho_c$. The current density $\vec{j}$ can be derived via Ampere's law, that is,

147 $$\vec{j} = \mu_0^{-1} \nabla \times \vec{B}. \quad (3)$$

148 We further summarize the magnetic rotation analysis method [*Shen et al., 2007*].
149 The rotation of a magnetic field vector is related to the tensor gradient of the magnetic
150 unit vector $\vec{b}$, i.e., $\nabla_j b_i$, where the subscript Latin index i or j (=1,2, and 3)
151 denotes the three components (x, y, and z). The square of the magnetic rotation rate

along an arbitrary direction $\vec{e}$ is

$$I^{(e)} = |(\vec{e}\cdot\nabla)\vec{b}|^2 = e_i e_j (\nabla_i b_l \nabla_j b_l) = e_i e_j S_{ij}, \quad (4)$$

Where $S_{ij} = \nabla_i b_l \nabla_j b_l$, which is named as the magnetic rotation tensor for convenience. By rotating the coordinate system, the magnetic rotation tensor can be diagonalized to obtain its eigenvalue $e^{(l)}(l=1,2,3)$ and the corresponding eigenvector μ_1, μ_2 and μ_3 ($\mu_1 \geq \mu_2 \geq \mu_3 \geq 0$). Then (4) can be expressed as

$$I^{(e)} = e_i e_j \mu_l e_i^{(l)} e_j^{(l)} = \mu_l (\cos\alpha_l)^2 = \mu_1 (\cos\alpha_1)^2 + \mu_2 (\cos\alpha_2)^2 + \mu_3 (\cos\alpha_3)^2. \quad (5)$$

Here α_l ($l=1,2,3$) are angles between $\vec{e}$ and the three eigenvectors $e^{(l)}(l=1,2,3)$, respectively. As shown by the formula (5), the magnetic field vector rotates at the largest rate at the $e^{(1)}$ direction.

3. Cases of RD structure in the magnetopause boundary layer

When the IMF is southward, magnetic reconnection may occur at the dayside magnetopause, then forming a RD structure. This allows the transfer of solar wind energy, momentum and mass into the magnetosphere and changes the structure of the magnetic field and current system. We have found some related magnetopause crossing events using MMS data and identify the RD structure at the magnetopause by the following criterion.

(1) The plasma beta (the ratio between the sum of ion thermal pressure and electron thermal pressure and the magnetic pressure) is much larger than 1 during the magnetopause crossing.

(2) The normal component of the magnetic field in the boundary layer is not zero

while the tangential component changes direction.

In this section, we present two typical cases which we identified to be RDs to illustrate the detailed features.

3.1 Event 1: December 8th 2015

The magnetopause crossing on 8 December 2015 is around 00:06:08 UT. Figure 1 shows GSE X-Z plane projection of the MMS orbit. We can see the MMS is crossing the magnetopause near the subsolar point. The event occurs during geomagnetic quiet periods and under southward IMF. The three components of IMF in GSM coordinates are (-4.45, -0.26, -2.23) nT and the clock angle of IMF during this crossing is 173.35^{o}. The position of the four spacecraft during this crossing is as follows: MMS1 (9.022, -3.889, -0.882) Re, MMS2 (9.024, -3.886, -0.882) Re, MMS3 (9.025, -3.889, -0.881) Re, MMS4 (9.024, -3.889, -0.883) Re. The four spacecraft are very close to each other so that we can use the curvature calculation [*Shen et al., 2003*] and magnetic rotation analysis [*Shen et al., 2007*] methods properly.

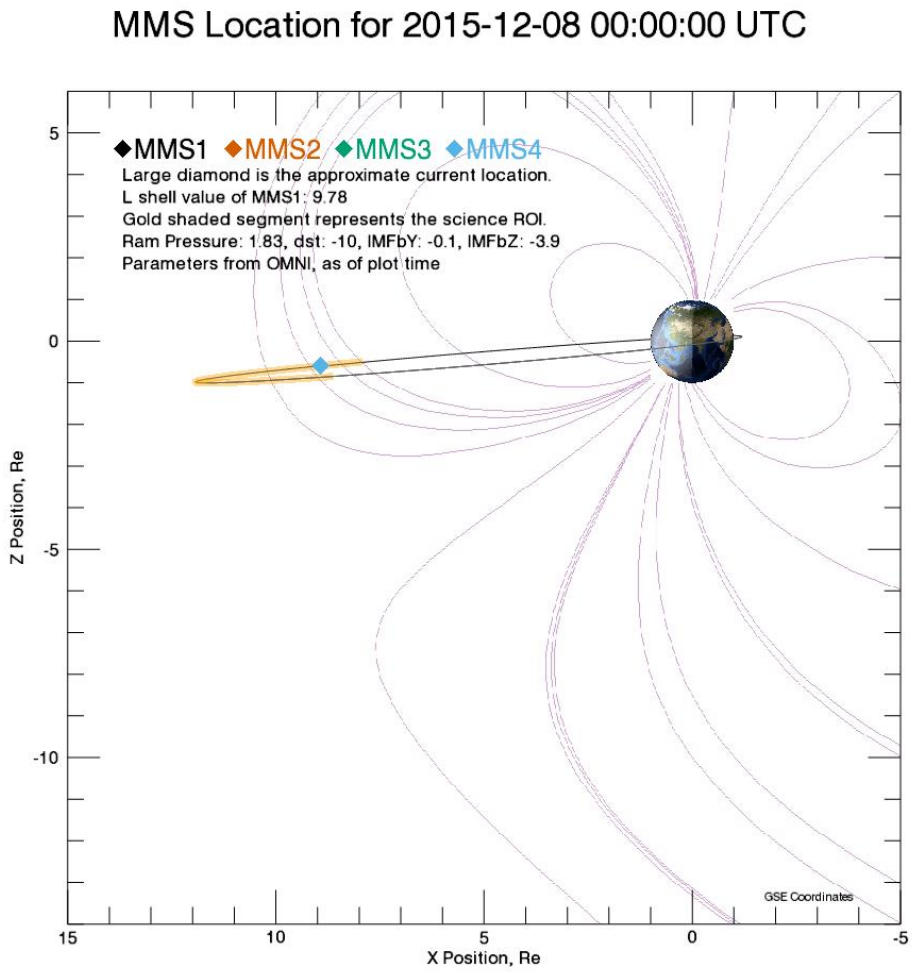

188

189 Figure 1. The MMS position projected into the XZ plane at 00:00:00 UT on

190 December 8th 2015. Adopted from MMS science data center historical orbit plots.

191

192 Figure 2 displays the hodogram of magnetic field of the LMN components in

193 boundary normal coordinates for the identified RD on December 8th 2015. In the

194 hodogram of BN-BM and BN-BL, we can see that it is almost a vertical line,

195 indicating that BN component is constant and estimated to be ~ -2 nT, which is

196 consistent with the general description of RD structure in the classical theory

197 [*Sonnerup et al., 1981*]. However, there is a slight rotation as shown in Figure 2a. We

suggest that this RD may be not a strictly one-dimensional structure, but a three-dimensional one. In the hodogram of BM-BL, there is an obvious rotation. It means that the magnetic field vector has a distinct rotation. We can conclude that the normal component of the magnetic field for this RD is constant and not zero while the tangential component rotates by some angle.

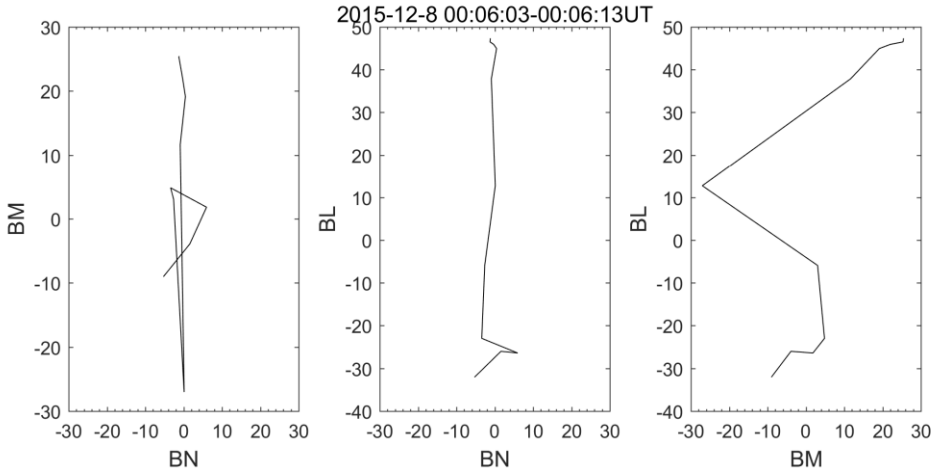

Figure 2. The hodogram of magnetic field of the LMN components in boundary normal coordinates for the identified RD on December 8th 2015.

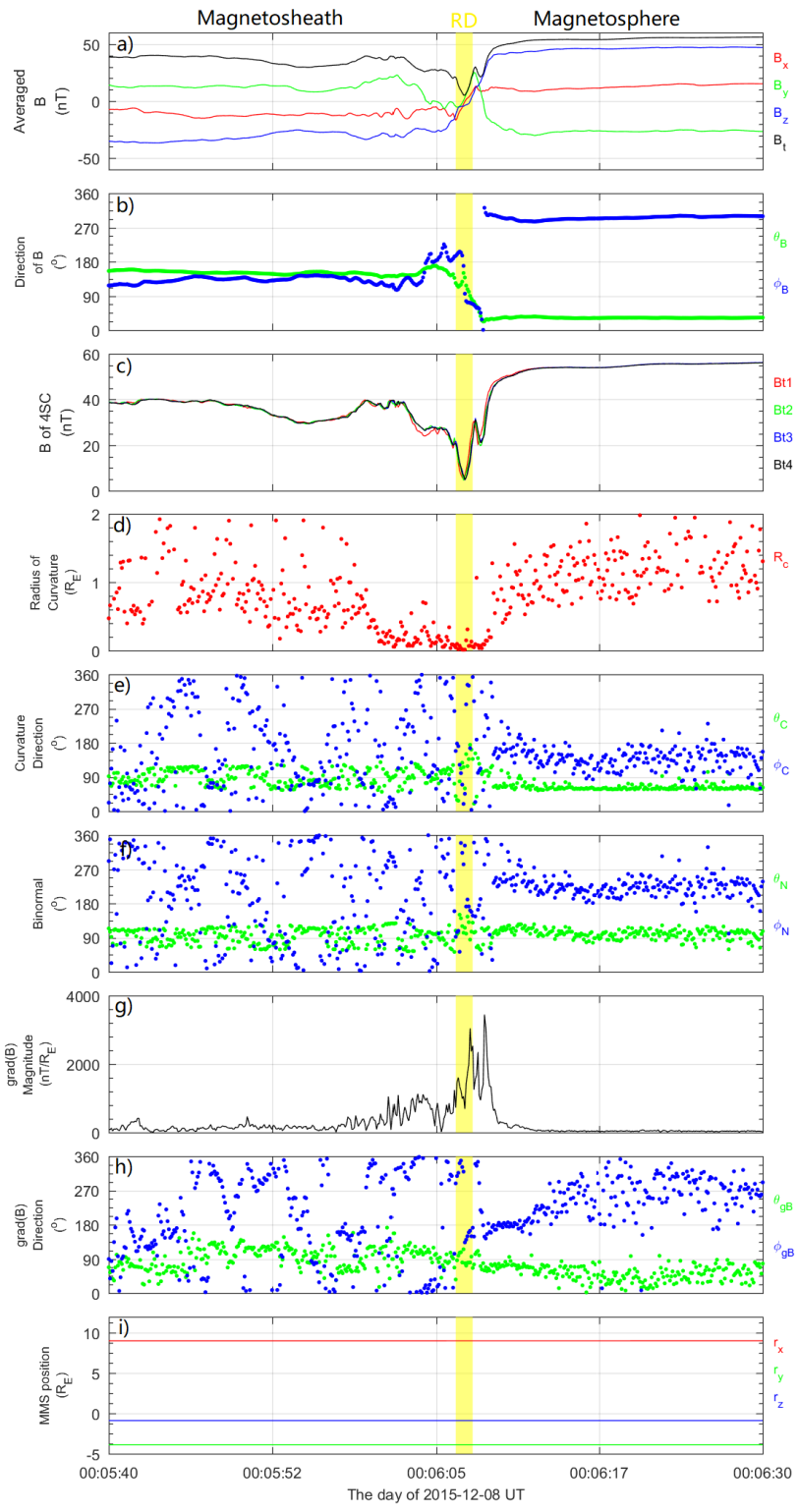

206

207 Figure 3. The structure of the magnetopause boundary layer during one MMS

208 crossing event on December 8th 2015. a) the magnetic field at the center of MMS

209 tetrahedron as are estimated with the average of those at the four S/C; b) the direction

angle of the magnetic field at the center of MMS tetrahedron; c) the magnetic field strengths observed by the 4 S/C of MMS; d) the radius of curvature of the magnetic field lines (MFLs); e) the direction angles of the curvature of the MFLs; f) the direction angles of the normal of the osculating plane, or the binormal; g) the value of the gradient of magnetic field strength; h) the directional angle of the gradient of magnetic field strength; i) the positions of MMS tetrahedron. The yellow shadow is the identified RD structure crossing.

Figure 3 illustrates the structure of the magnetic field as observed by MMS in the interval between 00:05:40 and 00:06:30 UT on December 8th 2015. The yellow shadow is the identified RD structure crossing. We can see that the topological structure of the magnetic field changes greatly and the magnetic field direction rotates obviously as the spacecraft crossing the RD. Figure 3e shows that the direction angle of MFL during RD crossing changes from ~（116.20°,19.42°） to ~（150.38°,281.21°）.There is a minimum value of the magnetic strength (not zero) during the RD crossing, indicating that MMS may be located near the magnetic X-line on the dayside magnetopause. We can see that the MMS spacecrafts take a very short interval crossing the identified RD region, which indicates that the RD structure is very thin. As shown in Figure 3d, the radius of curvature of the MFLs for this RD crossing is rather small with a minimum value $R_{cmin} \approx 0.41R_e$. The magnitude of the gradient of magnetic strength has a minimum value in the RD and reaches a maximum value in the magnetopause boundary layer. In Figure 3h, we can see that

the polar angle of the gradient of magnetic strength fluctuates around 90°, indicating the gradient of magnetic strength is approximately on the X-Y plane. The minimum value of the radius of curvature appears simultaneously with the minimum magnitude of the gradient of magnetic field strength during the crossing. The two sides of RD structure have distinct features. The analyses above imply that the MFLs are crossing the RD and connect the magnetosheath and magnetosphere, and the magnetopause is open here. We also can find that RD usually occurs closer to the magnetosheath side on the dayside magnetopause.

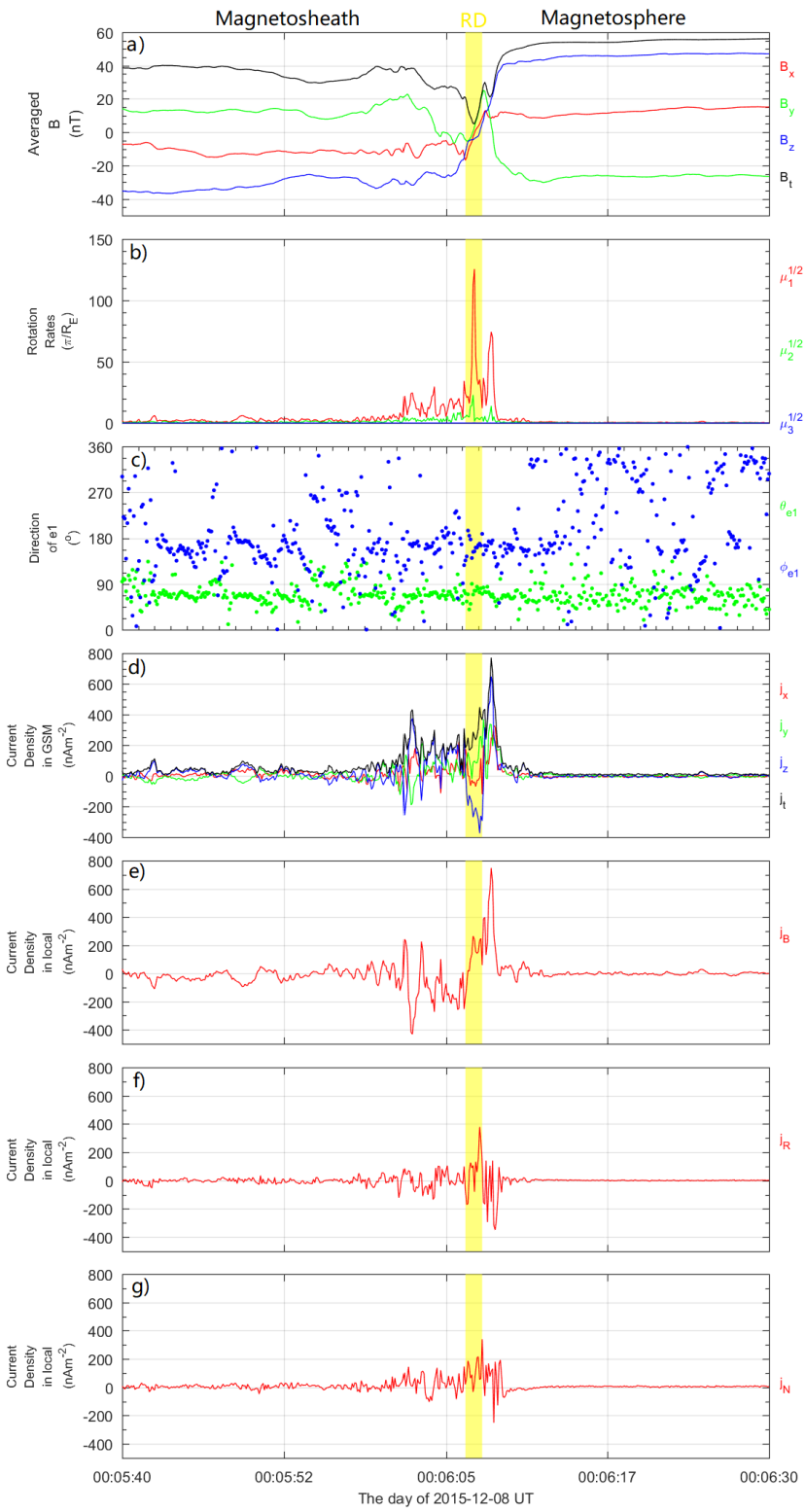

Figure 4. The magnetic field rotation features and current distribution when the MMS spacecraft are crossing the magnetopause on December 8th 2015. a) The magnetic field at the center of MMS tetrahedron as are the average of those at the four S/C; b)

The maximum, medium and minimum rotation rates of the magnetic field; c) the directional angles of the first eigenvector corresponding to the maximum rotation rate; d) The three components of the current density in GSM coordinates; e) The field-aligned component of the current density in the local natural coordinates; f) The component of the current density along the curvature in the local natural coordinates; g) The component of the current density along the binormal in the local natural coordinates.

Using the MMS 4-point measurements, we have calculated the magnetic rotation properties and current density distribution in the RD structure, as shown in Figure 4. By applying the magnetic rotation analysis (MRA) method (*Shen et al., 2007)*, we can obtain the maximum, medium and minimum rotation rates of magnetic field along three characteristic directions, just as shown in Figure 4b. During the entire magnetopause crossing, the rotation rate has a maximum value near the RD crossing, which is about $125.5\pi / R_e$, indicating that the magnetic field direction has the largest rotation at the RD structure. Then we can estimate RD's thickness by using an approximate formula $h = \pi / \mu_1^{1/2}$, that is approximately $7.97\times10^{-3} R_e$ (several ion inertial length), indicating that the RD at the dayside magnetopause is very thin. In addition, we can see that the maximum rotation rate is almost 6 times larger than the medium rotation rate and much larger than the minimum rotation rate. Therefore, the RD can be approximated as a one-dimensional structure. The normal of the RD can be estimated by the first eigenvector as shown in Figure 4c which is corresponding to the

maximum rotation rate, that is（76.64°,153.85°）. Figure 4d-4g present the current density deduced from the magnetic field measurement in GSM coordinates and local natural coordinates, respectively. We can see that the current density is relatively concentrated and has a maximum value (more than 600 $nA \cdot m^{-2}$) when crossing the magnetopause boundary layer. From the current density component in local natural coordinates (Figure 4e), we can find that the field-aligned component (also the Z component in GSM coordinates) of the current density is dominant. It means that the magnetic field is generally force-free in the magnetopause boundary layer. However, the maximum value of current density doesn't appear in the RD structure but out of it in the magnetopause boundary layer near the magnetosphere.

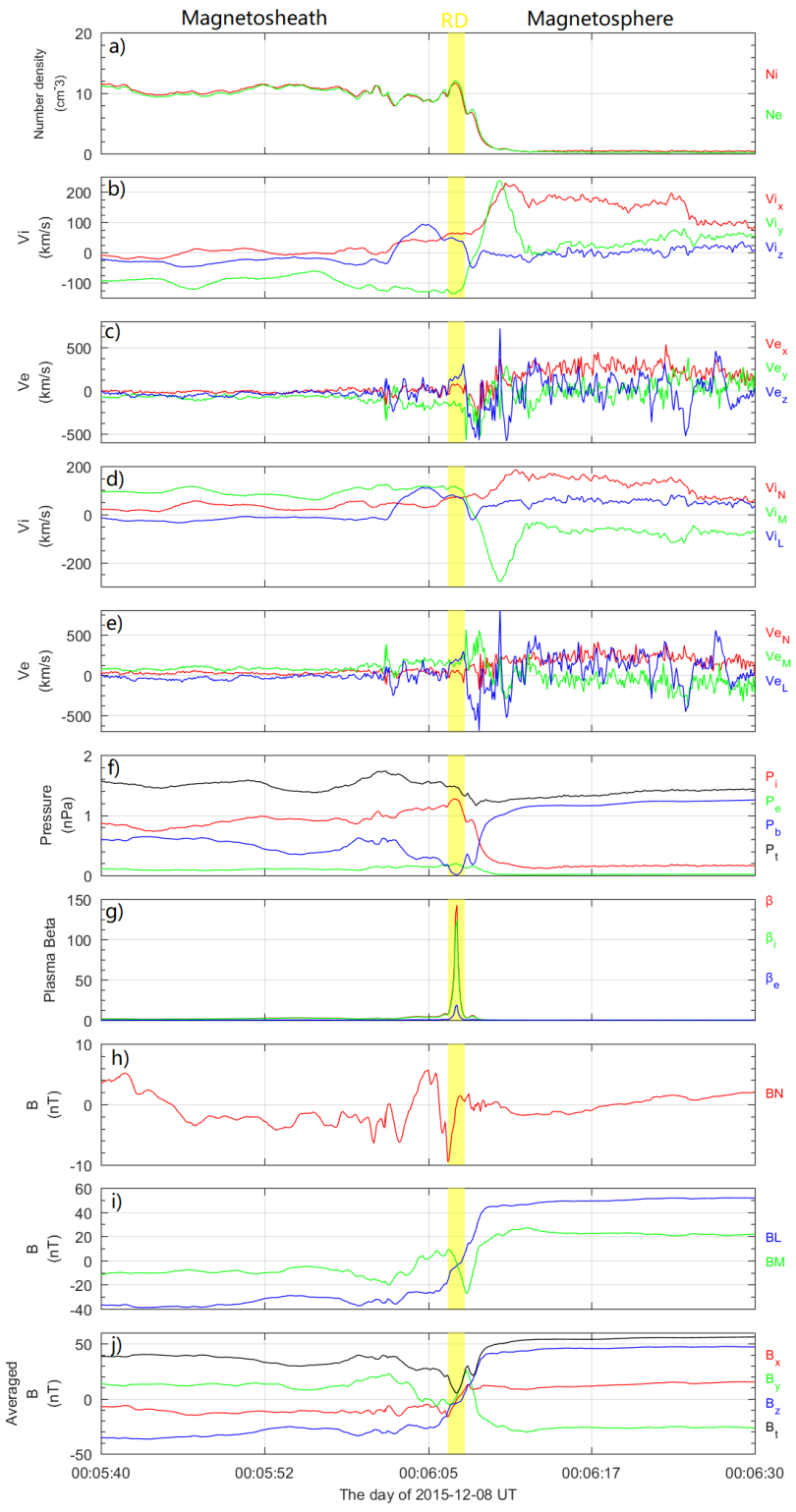

276

277 Figure 5. Illustration on the plasma parameters combined with the magnetic field

278 measurement during magnetopause crossing on December 8th 2015. a) The ion and

279 electron number density; b) The ion velocity in GSM coordinates; c) The electron

velocity in GSM coordinates; d) The ion velocity in Boundary normal coordinates; e) The electron velocity in boundary normal coordinates; f) The ion thermal pressure, electron thermal pressure, magnetic pressure and the total pressure; g) The plasma beta (the ratio between the sum of ion thermal pressure and electron thermal pressure and the magnetic pressure), ion plasma beta and electron plasma beta; h) The normal component of magnetic field in boundary normal coordinates (LMN); i) The other two components of magnetic field in LMN; j) The magnetic field at the center of MMS tetrahedron as are the average of that at the four S/C.

Figure 5 shows the plasma measurements in the interval when the MMS constellation is crossing the magnetopause on December 8th 2015. The spacecraft enter the RD (yellow shadow) at 00:06:06 UT, then about 1 second later they enter the magnetopause boundary layer, and finally enter the magnetosphere at 00:06:10 UT. We can see that the ion and electron number densities are basically unchanged before and after crossing the RD, however, there is a small density peak in the RD center. When the spacecraft are crossing the magnetopause boundary layer, there is a sharp decrease in the number density, and finally it becomes very slight and stable as MMS constellation enters the magnetosphere. Figure 5b-5e presents the ion and electron velocity in GSM coordinates and boundary normal coordinates, respectively. It is obvious that the ion and electron velocity are stable when the spacecraft crosses the RD, while there are sharp fluctuations during the magnetopause boundary layer crossing. The signatures of high-speed flow ($v_{ez} > 500 km/s$), large current density

magnitude (over $600nA \cdot m^{-2}$) and large amplitude electric field ($\sim 90mV/m$, not shown) during the magnetopause crossing indicate that the spacecraft are located in the reconnection outflow region and not far from the reconnection X-line. The magnitude of Z component of the electron velocity has a maximum and is negative, indicating that the spacecraft is crossing the outflow region southern of the reconnection X-line. The ion and electron thermal pressure has almost the same variations with the number density while the magnetic pressure shows a minimum during RD crossing. The total pressure remains relatively stable before and after the crossing of RD and magnetopause boundary layer. During the RD crossing, the plasma beta almost equals to the ion plasma beta ($\beta \approx \beta_i$). Besides we can see clearly that both β_i and β_e increase sharply and are much greater than 1, indicating that magnetic energy is rapidly converted into plasma thermal and dynamical energy during the RD crossing. We suggest this is a clear evidence that the RD structure is closely related with the magnetic reconnection processes. Figure 5h-5i gives magnetic field components in boundary normal coordinates. The most important feature of RD structure is the existence of the normal component of the magnetic field at the magnetopause. We can find that the normal component of the magnetic field is evident across the RD, although it is relatively small. Besides, B_L component has an obvious reverse from negative to positive across the boundary.

Some characteristics of the RD in the magnetopause are revealed from the above analysis on magnetopause crossing event on December 8th, 2015. RD occurs in the magnetopause and is closer to the magnetoshealth side. It is possibly caused by the

asymmetric magnetopause reconnection [*Cassak and shay, 2007*]. There is a minimum value of magnetic field strength within the RD. In the RD, magnetic field direction rotates severely and the radius of curvature of MFLs has a minimum value. The MFLs are about lying in the RD in the magnetopause because the minimum value of the radius of curvature of the MFLs is much larger than the thickness of the RD layer. The field-aligned current dominates in the RD.

3.2 Event 2: January 9th 2017

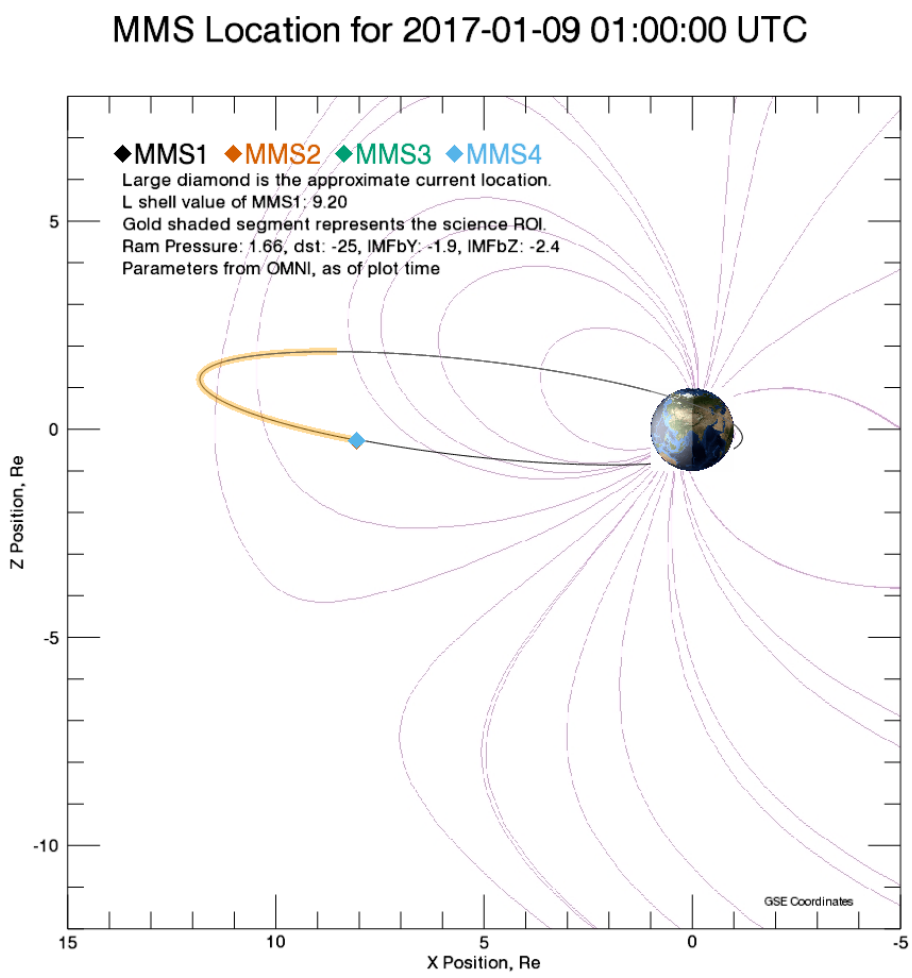

Figure 6. The MMS position projected into the XZ plane at 01:00:00 UT on January

9th 2017. Adopted from MMS science data center historical orbit plots.

The second event we show is the magnetopause crossing at 01:20:30 - 01:21:30 UT of 9th January 2017. Figure 6 is the MMS orbit projected into the XZ plane on January 9th 2017. Just as the first event on 8th December 2015, MMS crossed the magnetopause on dayside subsolar region. During the interval of crossing, IMF is southward. The three components of IMF in GSM coordinates are (3.34, -1.34, -1.19) nT. The clock angle of IMF during this crossing is about 131.61^{o}. The separation between the four spacecrafts is very small so that we can apply the curvature calculation of MFL and magnetic rotation analysis properly.

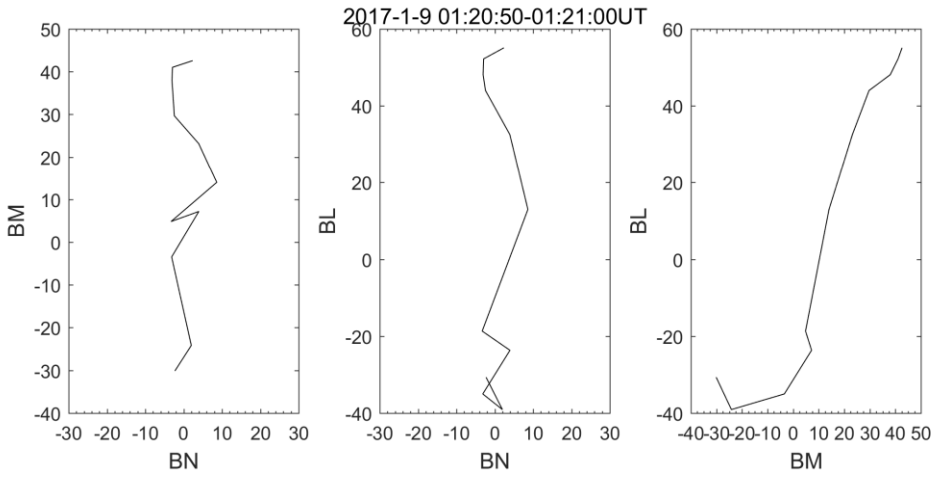

Figure 7. The hodogram of magnetic field of the LMN components in boundary normal coordinates for the identified RD on January 9th 2017.

Just as event 1, here we show the hodogram of magnetic field of the LMN components in boundary normal coordinates for the identified RD on January 9th 2017 in Figure 7. In the hodogram of BN-BM and BN-BL, we can see that it is approximately a vertical line, indicating that BN component is almost keeping

unchanged, which is also consistent with the general description of RD structure in the classical theory although it is rather small. In the hodogram of BM-BL, there is a clear rotation. We can conclude that the normal component of the magnetic field for the RD is close to constant and not zero while the tangential component rotates some angle.

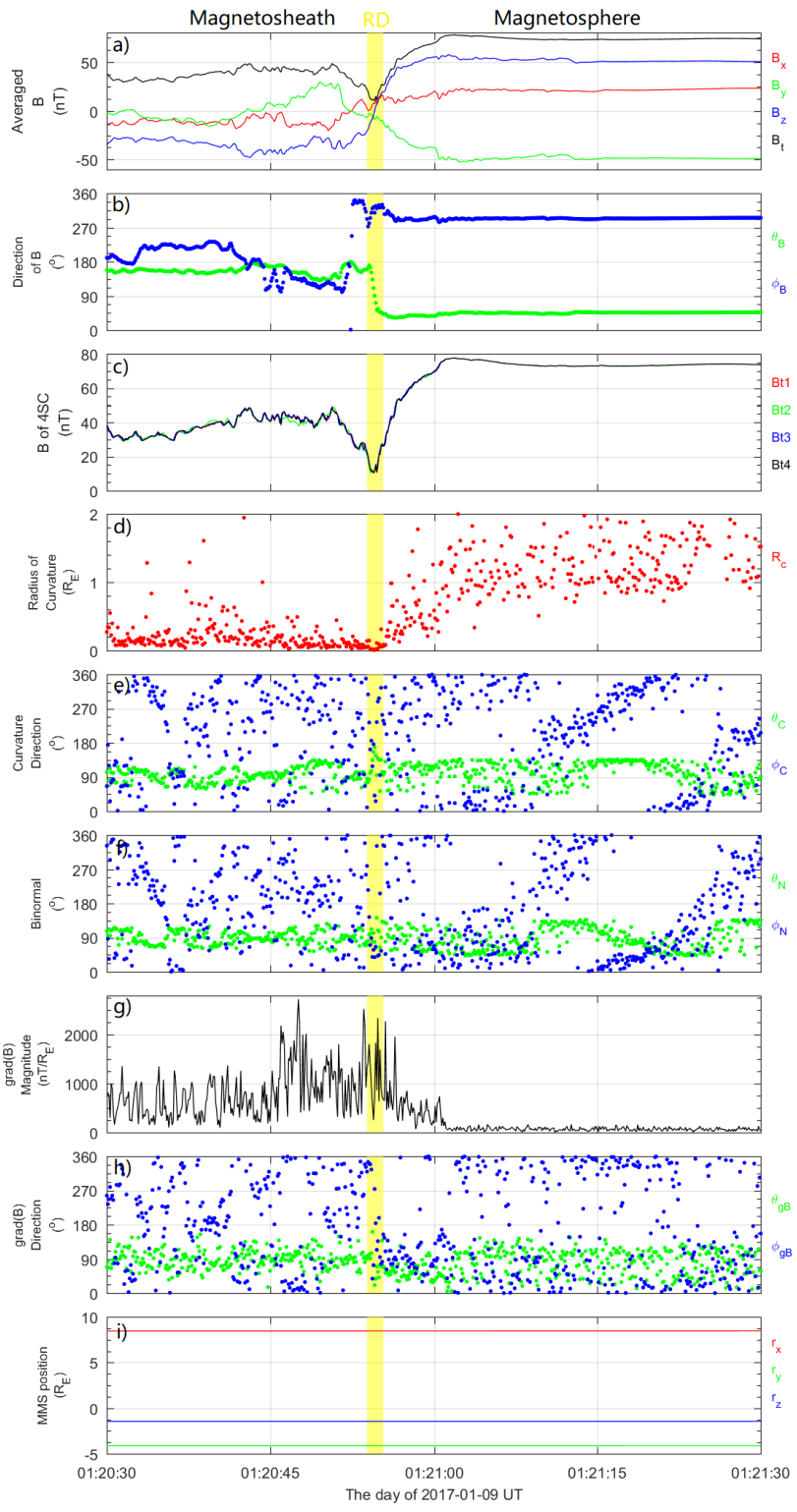

Figure 8. The structure of the magnetopause boundary layer during one MMS crossing event on January 9th 2017. The format of the figures and the instruction are the same as that of Figure 3.

Figure 8 shows the magnetic field observations of MMS in the interval between 01:20:30 and 01:21:30 UT on January 9th 2017. The yellow shadow is the identified RD structure crossing. The spacecraft pass through the magnetopause from the magnetosheath to the magnetosphere region during ~01:20:55 UT to ~01:21:00 UT. During the RD crossing, the magnetic field magnitude has a minimum value and the direction of magnetic field has changed significantly, from ~（134.40°,118.52°） to ~（168.82°,41.38°）. Besides, the Z compontent of the magnetic field also shows an obvious reversal from negative to positive. The RD crossing time is very short indicating the RD structure is very thin. The radius of curvature of the MFLs for this RD crossing has a minimum value, and the magnitude of the gradient of the magnetic field strength has a minimum value during the RD crossing. These two features appear almost simultaneously. All the characteristics demonstrate it is a classical RD structure. The normal of the magnetopause can be determined from the direction of the gradient of the magnetic strength, which is about（37.42°,183.89°）.

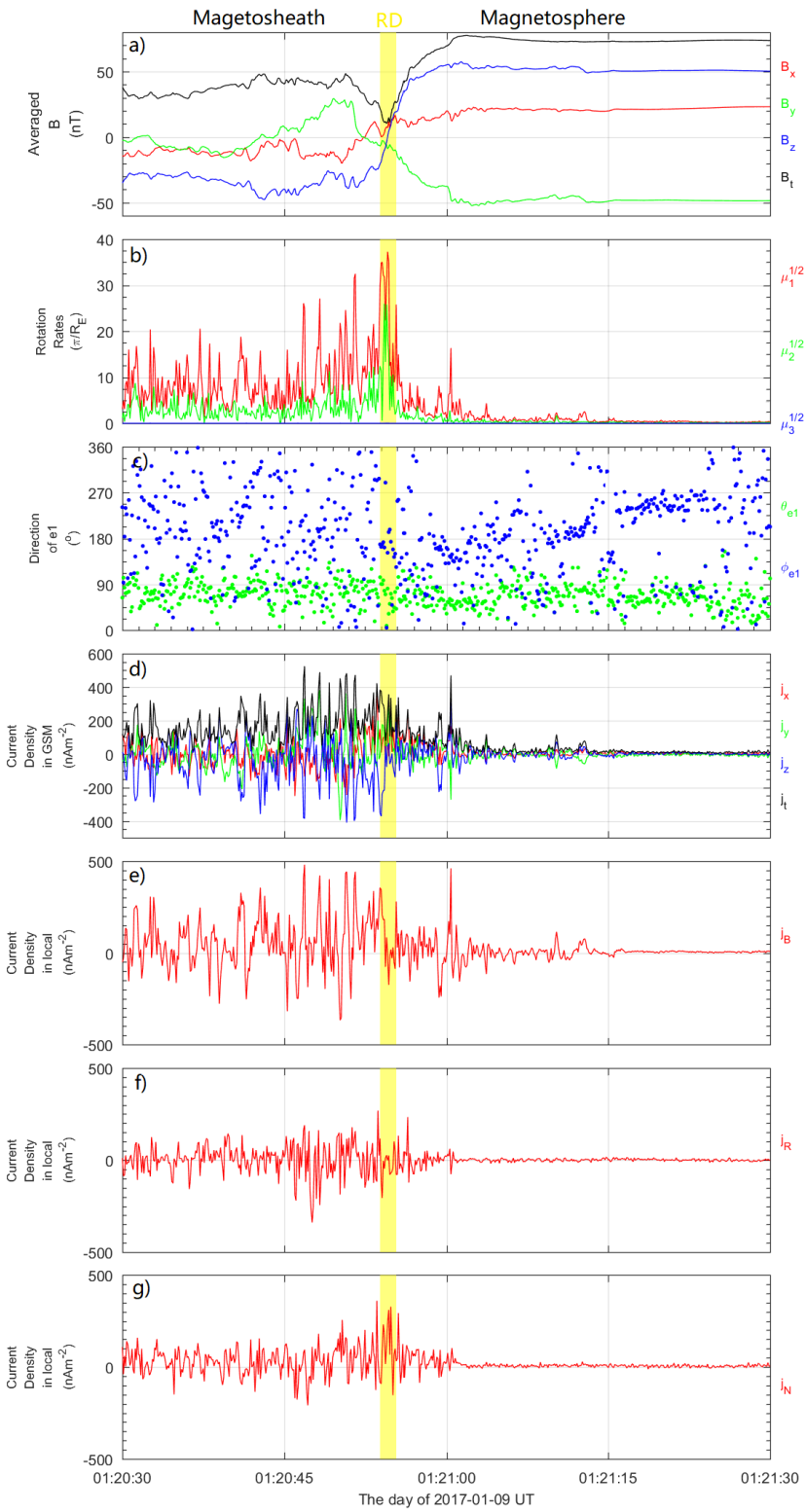

Figure 9. The magnetic field rotation features and current distribution when the MMS spacecraft are crossing the magnetopause boundary layer on January 9th 2017. The format of the figures and instruction are the same as those of Figure 4.

Figure 9 shows the magnetic field rotation and current distribution analysis in detail during this magnetopause crossing on January 9th 2017. We calculate the magnetic field rotation rate by MRA and find that the maximum rotation rate ($\sim 37.3\pi/R_e$) also occurs when the spacecraft passes through the RD structure. Using the simple formula $h = \pi / \mu_1^{1/2}$, we can get the thickness of RD which is approximately $0.0268R_e$, indicating that this RD is very thin. The relative magnitude of the maximum, medium and minimum magnetic field rotation rates manifests that this RD can also be approximated as a one-dimensional structure. The normal of the RD can also be estimated by the first eigenvector, that is（32.12°,192.38°）, which is about the same as that of the magnetopause. The current density deduced from the magnetic field measurement is shown in Figure 9d-9g. The current density in the magnetosheath fluctuates dramatically and much larger than that in the magnetosphere. During the RD crossing, the magnitude of current density has a larger value relative to that in the magnetopause boundary layer crossing and the dominated component is the Z-component in GSM coordinates. Due to the large fluctuations of current density in GSM coordinates as deduced from the magnetic field measurement, the distribution in the local natural coordinates gets distorted.

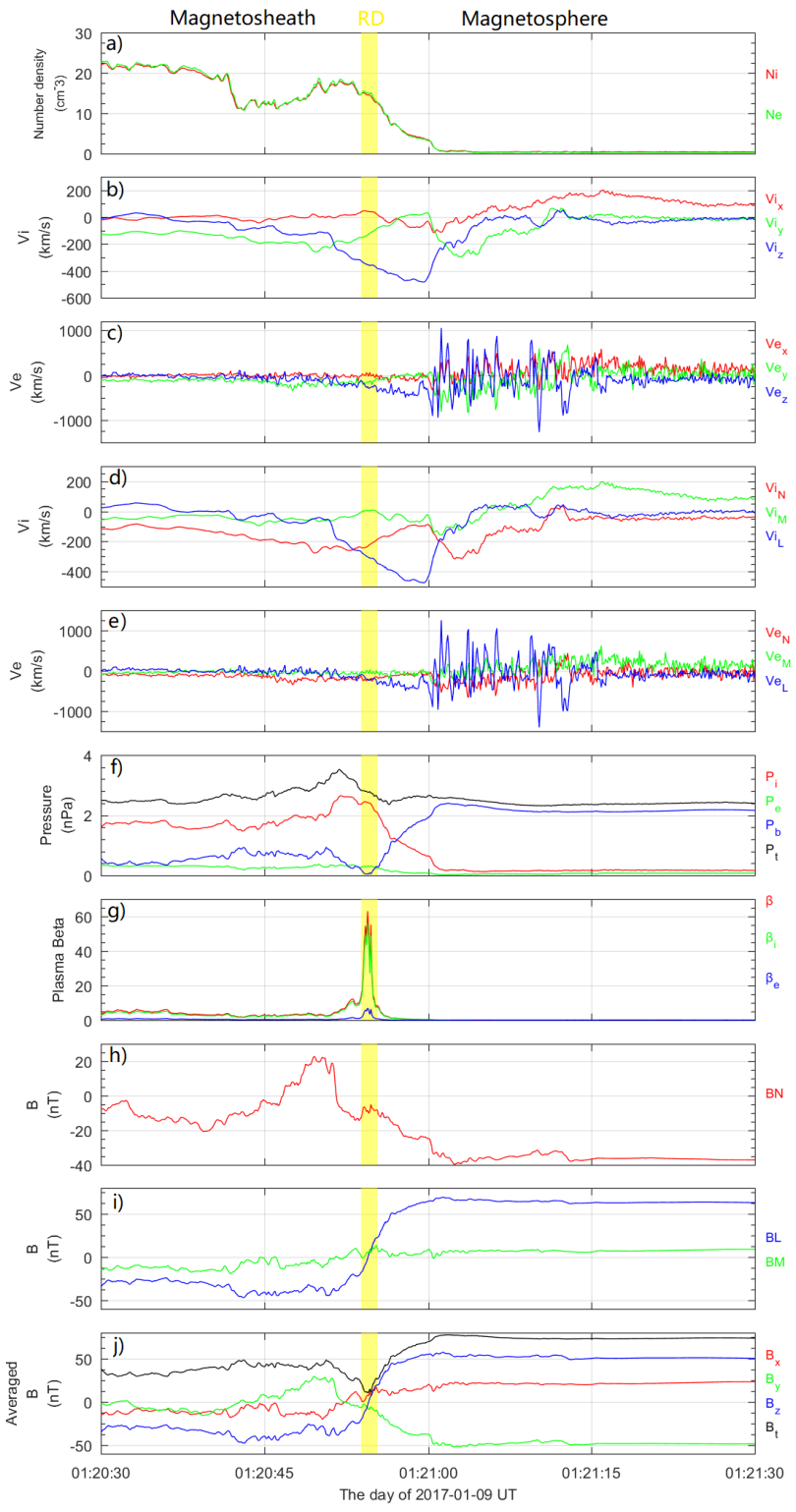

Figure 10. The plasma parameters combined with the magnetic field measurement during magnetopause boundary layer crossing on January 9th 2017. The format of the figures and the instruction are the same as those in Figure 5.

We present the plasma measurement during January 9th 2017 crossing in Figure 10. Across the RD structure, the ion and electron number densities are basically unchanged. After the RD crossing, the ion and electron number density drop significantly until entering the magnetosphere. The velocities of the ions and electrons in GSM coordinates and boundary normal coordinates (LMN) are shown in Figure 10b-10e. During the RD crossing, the velocities of the ions and electrons do not change much. In the magnetospheric boundary layer, however, there is large southward component in GSM as well as L component in LMN ($V_{iL} < -400 km/s$) of the ion velocity. It indicates that this RD structure is associated with magnetic reconnection in the dayside magnetopause and is located southward of reconnection X-line. The ion and electron thermal pressure (p_i and p_e) decreases while the magnetic pressure (p_b) increases during the magnetopause crossing. It is shown that the total pressure (p_t), which is composed of the ion and electron thermal pressures and the magnetic pressure, remains unchanged during the magnetopause transition, in consistence with the pressure balance condition. When crossing the RD, the plasma beta is dominated by ion beta, that is $\beta \approx \beta_i$, because the ions are generally hotter than electrons. It is noted that the plasma beta shows a sharp peak in the RD. Figure 10h shows that the normal component of the magnetic field in LMN remains almost unchanged and is not zero for the RD crossing, while the L component of magnetic field (tangential component) changes evidently from negative to positive.

In brief, during this magnetopause crossing on January 9th 2017, RD structure

426 also appears near the magnetosheath side of the magnetopause. There is a minimum
427 value of the magnetic strength within the RD. The largest rotation rates of the
428 magnetic field direction and the minimum value of the radius of curvature of MFLs
429 appear in the RD. Similarly, the minimum value of the radius of curvature of MFLs is
430 always larger than the thickness of RD.
431
432 **4. Statistical analysis of the RD at the magnetopause boundary layer**
433 Using the magnetic field measurement from FGM instrument [*Russell et al.,*
434 *2014*] and the plasma parameter measurement from FPI instrument [*Torbert, et al.,*
435 *2015; Pollock et al., 2016*] on board MMS mission during 2015 to 2018, we totally
436 select 22 examples of RDs through the visual analysis just as shown in Section 3. We
437 summarize these examples in the Table 1 below. We find that the time for the
438 spacecraft to cross the RD structure is very short, which implies RD is usually very
439 thin. The IMF is mostly southward (16 out of 22). When the IMF is southward,
440 magnetic reconnection is more likely to occur in the dayside low latitude boundary
441 layer. There are also some cases of RD observations (6 out of 22) during northward
442 IMF. It is indicated that possibly the RD is closely related with magnetopause
443 reconnection, including the anti-parallel reconnection and component reconnection.
444 The radius of curvature of the MFL during RD crossing is within the range of
445 0.03~0.62 R_e . During the RD crossing, field-aligned current is the dominant
446 component, with the ratio between parallel current and perpendicular current of
447 mostly larger than 2. The thickness of the RD is with the range of 0.00079 - 0.06917

R_e, that is 5 - 440 km.

Table 1. Detailed RD structure descriptions of 22 examples from 2015 to 2018.

Case	Time (UT)	Position (GSM:Re)	IMF (GSM:nT)	IMF clock angle	Dst(nT)	Rc (Re)	thickness (10^(-3)Re)	jt(nAm²)	$\|j_{//}\|$(nAm²)	$\|j_{\perp}\|$(nAm²)	$\|j_{//}/j_{\perp}\|$
2015.10.30	05:15:41~05:15:51	(10.1, 2.4, -1.4)	(-5.69,-4.86,1.38)	285.85	3	0.56	69.14	311.51	217.35	150.09	5.94
2015.11.04	03:07:08~03:07:18	(9.2, 0.7, -0.5)	(-2.46,4.35,1.21)	75.56	-35	0.06	8.02	373.86	272.44	142.93	4.58
2015.11.13	04:02:43~04:02:53	(10.6, 0.5, -0.7)	(-2.78,0.5,-1.03)	154.11	-16	0.06	8.63	279	237.24	92.64	7.93
2015.12.03	02:38:35~02:38:45	(10.8, -2.4, -0.6)	(-3.56,1.84,-3.51)	152.34	-11	0.06	4.07	436.49	139.57	281.78	1.47
2015.12.08	00:06:03~00:06:13	(9.0, -3.9, -0.9)	(-4.45,-0.26,-2.23)	186.65	-10	0.41	7.97	217.52	154.64	86.12	6.76
2015.12.08	10:21:45~10:21:55	(10.9, 0.8, -1.3)	(-3.63,1.78,0.76)	69.37	-12	0.16	3.31	319.59	212.97	156.65	25.6
2015.12.20	23:35:52~23:36:02	(8.9, -5.4, -1.7)	(-4.98,-2.01,-18.89)	186.07	-151	0.31	26.92	94.07	53.64	44.19	6.24
2015.12.28	22:19:01~22:19:11	(7.7, -6.3, -2.3)	(-3.69,2.23,-1.74)	127.96	9	0.41	8.16	189.12	144.79	71.68	5.64
2016.01.01	22:00:27~22:00:37	(7.4, -6.7, -2.6)	(4.73,-0.96,0.53)	298.90	-29	0.41	8.15	164.86	85.84	79.93	23.45
2016.11.28	07:36:50~07:37:00	(10.0, 2.8, -1.2)	(-3.69,0.95,-0.79)	129.75	-8	0.17	10.4	215.91	157.83	89.11	8.94
2016.12.02	08:49:13~08:49:23	(10.8, 3.4, -1.1)	(-4.88,0.71,-2.19)	162.04	1	0.2	0.79	287.48	156.03	102.49	19.5
2016.12.13	13:41:30~13:41:40	(10.5, 4.8, 0.3)	(3.17,-0.94,1.8)	332.43	4	0.13	8.79	237.7	162.12	90.78	62.71
2016.12.17	04:15:28~04:15:38	(9.7, -0.8, -0.3)	(2.79,-1.26,-0.92)	233.89	11	0.03	5.62	361.49	142.87	234.16	3.49
2016.12.22	14:36:00~14:36:10	(9.9, 3.9, 1.2)	(-5.39,-1.84,-3.32)	209.00	-23	0.33	5.61	273	179.85	138.15	2.52
2016.12.23	06:13:26~06:13:36	(11.3, -0.4, 0.2)	(-2.51,2.59,-3.21)	141.10	-18	0.06	6.14	413.86	320.1	167.72	5.37
2017.01.07	13:47:52~13:48:02	(9.7, 1.6, 1.8)	(-2.71,-1.24,-3.12)	201.67	-17	0.09	7.81	484.77	221.78	220.76	3.87
2017.01.09	01:20:50~01:21:00	(8.4, -4.1, -1.4)	(3.34,-1.34,-1.19)	228.39	-25	0.2	26.84	204.26	131.07	74.37	3.21
2017.01.27	11:17:23~11:17:33	(9.8, -2.0, 1.9)	(-2.88,2.61,-0.01)	90.22	-14	0.13	7.1	261.65	124.42	122.95	2.84
2017.01.28	00:42:11~00:42:21	(8.1, -6.3, -2.5)	(-0.17,2.78,-1.11)	111.77	-10	0.27	6.41	263.27	149.2	144.18	5.29
2017.01.29	09:16:13~09:16:23	(10.5, -3.6, 1.6)	(?,0.6,-1.2)	153.43	-10	0.11	12.66	267.66	190.53	93.3	6.18
2017.01.30	08:15:43~08:15:53	(10.6, -4.4, 1.3)	(-0.21,3.9,1.32)	71.30	1	0.22	2.39	112.53	70.12	52.09	5.46
2018.11.12	04:11:15~04:11:25	(-0.8, 18.5, -0.2)	(?, -2.1, -2.4)	221.19	-9	0.62	5.7	52.07	35.21	17.92	18.2

Based on the above analysis, we depict the feature of the structure of RD at the dayside magnetopause in Figure 11. From top to bottom, we demonstrate the variations of the magnitude of magnetic field, the magnitude of gradient of the magnetic field strength, the radius of curvature, the maximum rotation rate of magnetic field and the current density. This illustration summarizes the characters of the magnetopause boundary layer with strong magnetic shear. All these features can be observed in the previous examples. The magnitude of magnetic field has a minimum value during the RD crossing, indicating that RD structure is closely associated with magnetic reconnection at the magnetopause. The magnitude of gradient of magnetic field strength has a minimum value during the RD crossing while there is a peak in the magnetopause boundary layer near the magnetosphere. During the RD crossing, there is a maximum rotation rate of magnetic field, a

466 minimum radius of curvature and a large enhancement of current density. The peak
467 value of the current density usually appears in the magnetopause boundary layer out
468 of RD. Another characteristic is that field-aligned current is dominated during the RD
469 crossing, which is not shown in Figure 11.
470

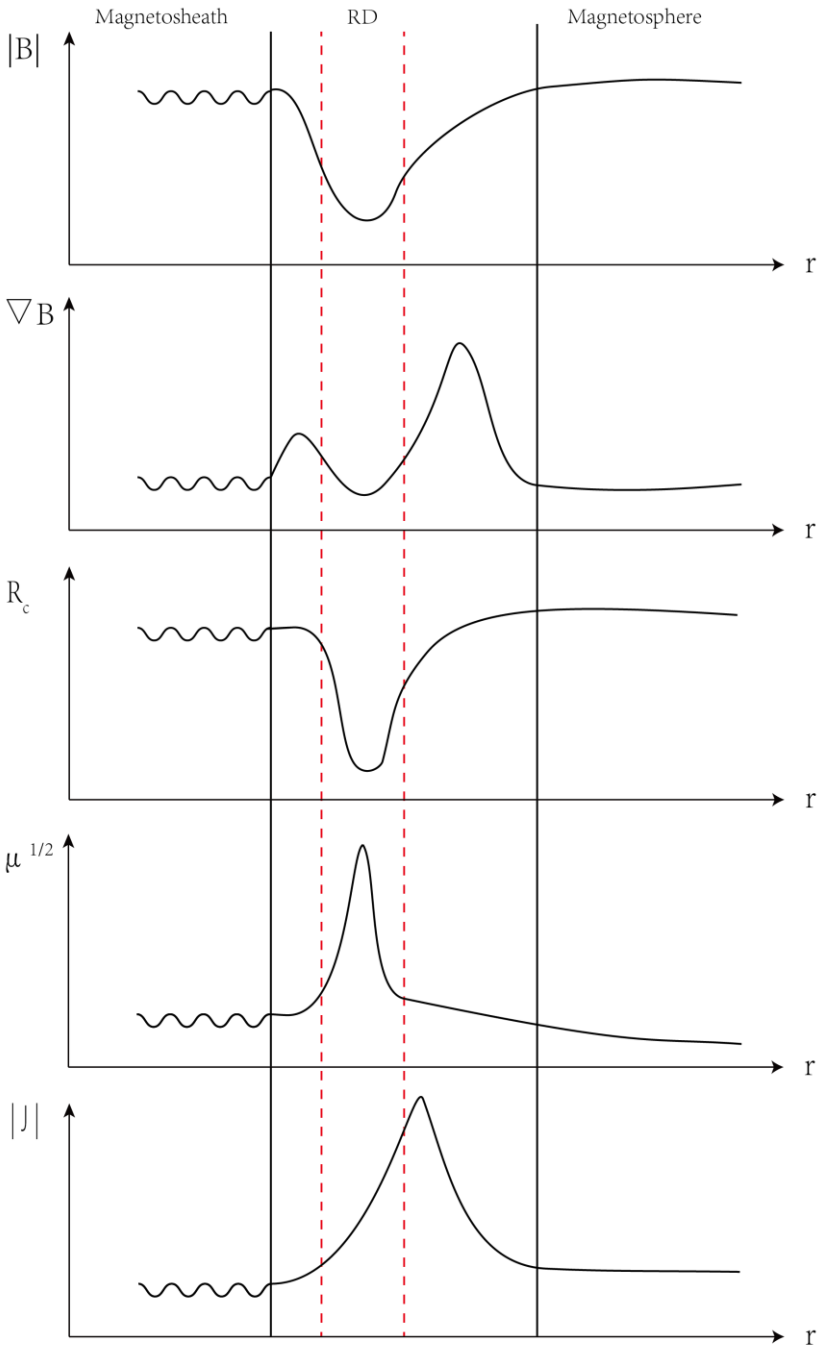

Figure 11. The feature of the structure of RD at the dayside magnetopause from magnetosheath side to magnetospheric side. From top to bottom: the variations of the magnitude of magnetic field, the magnitude of gradient of the magnetic field strength,

the radius of curvature, the maximum rotation rate of magnetic field and the current density. The region between the two solid vertical black lines represents the magnetopause boundary layer. The region between the two dashed vertical red lines represents the RD structure.

5. Discussion and conclusions

This research has verified that the magnetopause boundary layer contains a rotational transition layer or RD with certainty when the magnetic reconnection occurs in the low latitude dayside magnetopause. Previous investigations have confirmed the existence of the normal component of the magnetic field in the boundary layer as the magnetosphere is open, however, it is too small and may be smaller than the measurement error.

In this paper, using curvature calculation and magnetic rotation analysis method, the fine magnetic structure and current distribution deduced from the four-point MMS magnetic field observations as well as other plasma characteristics of the RD in the magnetopause have been investigated. It is indicated that the RD structure is very thin and its thickness is much smaller than 0.1 Re. During the RD crossing, the magnetic field has the largest rotation. The radius of curvature of MFLs in the RD is ~0.03-0.62 Re, while the thickness of RD is 0.00079 - 0.06917 R_e. Generally, the radius of curvature of MFLs in the RD is much larger than the thickness of RD. It means that the MFLs are partly lying on the RD. The calculation of the current density from magnetic field measurement shows that the current density is relatively concentrated

in the magnetopause boundary layer and field-aligned current dominates. The calculations show that the current density has a large enhancement during RD crossing and the peak current density usually appears in the magnetopause boundary layer near the magnetosphere. During RD crossing, both ion and electron velocities remain relatively stable. In the RD region, plasma beta is much larger than 1 and the magnetic strength has a minimum value. These features confirm that the formation of RD is closely associated with the magnetopause reconnection. As a result of reconnection, the two sides of magnetopause boundary layer can become linked to each other. Therefore, RD has special fine structure and is a key layer within the magnetopause for an open magnetosphere.

Acknowledgments

The authors are thankful to the entire MMS team for providing the MMS data (http://lasp.colorado.edu/mms/sdc/). OMNI Data used for the IMF condition and magnetic indices in this study are publicly available from the CDAWeb (https://cdaweb.gsfc.nasa.gov/cdaweb/istp_public/).This work was supported by National Natural Science Foundation of China (Grant No. 41704168, 41874190, and 11975086).

References

Aggson, T. L., P. J. Gambardella, and N. C. Maynard (1983), Electric Field Measurements at the Magnetopause, 1. Observation of Large Convective Velocities at Rotational Magnetopause Discontinuities, *J. Geophys. Res.*, *88*(A12), 10,000–10,010.

Burch, J. L., Moore, T. E., Torbert, R. B., & Giles, B. L. (2016). Magnetospheric Multiscale overview and science objectives. *Space Science Reviews*, 199(1 - 4), 5 – 21. https://doi.org/10.1007/s11214 - 015 - 0164 - 9.

Cassak, P. A., and M. A. Shay(2007), Scaling of asymmetric magnetic reconnection: general theory and collisional simulations, *Physics of Plasmas, 14*(10), 034702-034702-3.

Chou, Y.-C., and L.-N. Hau (2012), A statistical study of magnetopause structures: Tangential versus rotational discontinuities, *J. Geophys. Res.*, 117, A08232, doi:10.1029/2011JA017155.

Crooker, N.U., An evolution of antiparallel merging. *Geophys. Res. Lett.* **13**, 1063–1066, 1986.

Dungey J. W., Interplanetary magnetic field and the aurora zones, *Phys. Rev.*, **5**, 47-48, 1961.

Haaland, S., Runov, A., Artemyev, A., & Angelopoulos, V. (2019). Characteristics of the flank magnetopause: THEMIS observations. *Journal of Geophysical Research: Space Physics*, 124. https://doi.org/10.1029/2019JA026459.

Krauss-Varban, H. Karimabadi, and N. Omidi, Kinetic structure of rotational

563 discontinuities: Implications for the magnetopause, *J. Geophys. Res.*, **100**,
564 11981-11999, 1995.
565 Lee, L. C., L. Huang, and J. K. Chao, On the stability of rotational discontinuities and
566 intermediate shocks, *J. Geophys. Res.*, **94**, 8813-8825, 1989.
567 Levy, R. H., H. E. Petschek, and G. L. Siscoe, Aerodynamic aspects of the
568 magnetospheric flow, AIAA J., **2**, 2065, 1964.
569 Pollock, C., Moore, T., Jacques, A., Burch, J., Gliese, U., Saito, Y., et al. (2016). Fast
570 plasma investigation for Magnetospheric Multiscale. *Space Science Reviews*, 199, 331
571 – 406. https://doi.org/10.1007/s11214-016-0245-4.
572 Russell, C. T., Anderson, B. J., Baumjohann, W., Bromund, K. R., Dearborn, D.,
573 Fischer, D., et al. (2014). The Magnetospheric Multiscale magnetometers. *Space*
574 *Science Reviews*, 199, 189 – 256. https://doi.org/10.1007/s11214-014-0057-3.
575 Shen, C., X. Li, M. Dunlop, Z. X. Liu, A. Balogh, D. N. Baker, M. Hapgood, and
576 Xinyue Wang, Analyses on the Geometrical Structure of Magnetic Field in the
577 Current Sheet Based on Cluster Measurements, *J. Geophys. Res.*, 108, 1168, 2003.
578 Shen, C., X. Li, M. Dunlop, Q. Q. Shi, Z. X. Liu, E. Lucek, and Z. Q. Chen (2007),
579 Magnetic field rotation analysis and the applications, *J. Geophys. Res.*, 112, A06211,
580 doi:10.1029/2005JA011584.
581 Sonnerup, B. U. O., and B. G. Ladley, Magnetopause rotational forms, *J. Geophys.*
582 *Res.*, **79**, 4309, 1974.
583 Sonnerup, B. U. O., and B. G. Ladley, OGO-5 magnetopause structure and classical
584 reconnection, *J. Geophys. Res.*, **84**, 399, 1979.

585 Sonnerup, B. U. O., G. Paschmann, I. Papamastorakis, N. Sckopke, G. Haerendel, S. J.
586 Bame, J. R. Asbridge, J. T. Gosling, and C. T. Russell (1981), Evidence for magnetic
587 field reconnection at the Earth's magnetopause, *J. Geophys. Res.*, 86, 10,049–10,067.
588 Paschmann G, Haaland S, Phan T D, et al. Large-scale survey of the structure of the
589 dayside magnetopause by MMS[J]. *Journal of Geophysical Research*,
590 2018,123(3): 2018-2033.
591 Torbert, R. B., Vaith, H., Granoff, M., Widholm, M., Gaidos, J. A., Briggs, B. H., et al.
592 (2015). The electron drift instrument for MMS. *Space Science Reviews*, 199(1‐4),
593 283‐305. https://doi.org/10.1007/s11214‐015‐0182‐7
594